Published in final edited form as:

Adv Compos Hybrid Mater. 2018 March ; 1(1): 185–192. doi:10.1007/s42114-017-0002-5.

Polyvinylidene Fluoride (PVDF)/Polyacrylonitrile (PAN)/Carbon Nanotube Nanocomposites for Energy Storage and Conversion

Salem M. Aqeel[a,b], **Zhongyuan Huang**[a,c], **Jonathan Walton**[d], **Christopher Baker**[d], **D'Lauren Falkner**[a], **Zhen Liu**[d,*], and **Zhe Wang**[a,*]

[a]Chemistry Department, Xavier University of Louisiana, New Orleans, LA, 70125, United States

[b]Department of Chemistry, Faculty of Applied Science, Thamar University, P. O. Box 87246, Thamar, Yemen

[c]College of Chemistry and Chemical Engineering, Xinyang Normal University, Xinyang, 464000, China

[d]Department of Physics and Engineering, Frostburg State University, Frostburg, MD 21532-2303, United States

Abstract

Polyvinylidene fluoride (PVDF)/Polyacrilonitrile (PAN)/Multiwalled nanotubes functionalized COOH (MWNT-COOH) nanocomposites with different contents of MWNTs were fabricated by using electrospinning and solution cast methods. The interaction of the MWNTs with the polymer blend was confirmed by a Fourier transform infrared (FTIR) spectroscopy study. The dispersion of the MWNTs in the polymer blend was studied by scanning electron microscopy. The impedance and electrical conductivity of PVDF-PAN/CNTs in a wide frequency range at different temperatures have been studied. The effect of the concentration of the filler on the conductivity of the polymer composite was discussed. Nanocomposites based on PVDF/PAN and MWNTs as filler, show a significant enhancement in the electrical conductivity as a function of temperature.

Introduction

Polymer nanocomposites containing carbon nanotubes (CNTs) have involved extensive interest due to their electrical, physical and mechanical properties. The nano-structural elements can be used as nano-fillers and nano-reinforcements of advanced composite materials to improve the mechanical, thermal and impact-resistance properties[1–10]. Polyvinylidene fluoride (PVDF) and Polyacrylonitrile (PAN) independently have useful characteristics as the importan polymers in nanocomposites. It was determined that PAN has good process ability, flame resistance, resistance to oxidative degradation and electrochemical stability. PAN also has a high oxidative stabilization even at high temperature[11]. Moreover, PAN could provide a few important characteristics towards polymer electrolytes which could not be derived from PVDF[12]. PVDF has been extensively

Corresponding author: Z. Liu (zliu@frostburg.edu), Z. Wang (zwang@xula.edu).

studied as an important crystalline polymer for a broad range of applications, including, but not limited to, transducers[13], non-volatile memories[14,15], and electrical energy storage[16,17].

Nanocomposites, based on PVDF, PAN, and multiwalled nanotubes (MWNTs), have been under investigation recently. CNTs could improve thermal stability and Young's modulus of PAN/SWNT nanofibers[18,19]. As wide-used dielectric material, the effect of CNTs on the electric properties of PVDF and PAN have yet to be understood fully. The nanofibers of PAN/CNTs revealed a significant improvement in mechanical properties and thermal stability[18]. It has been shown that significant interactions occur between PAN chains and CNTs, which leads to higher direction of PAN chains during the heating process[20].

In order to obtain the consistent and uniform electric properties in one dimension, well-aligned and dispersed CNTs were desired in the host polymer. Electrospinning is a simple and low-cost method which could make CNTs embedded in a host, formed as a non-woven web.[21–24] The performance of CNTs prepared using this method relies on the distribution of fibers within. It was discovered that in the electrospinning process, CNTs could be aligned along the fiber axis. A high voltage was used in this technique to create an electrically charged jet of polymer solution or melt. The electric field reached a critical value at which the repulsive electric force overcame the surface tension of the polymer solution. The polymer solution was ejected from the tip to a collector. While traveling to the collector, the solution jet solidified or dried due to the fast evaporation of the solvent and was deposited on a collector to leave a polymer fiber[25–29].

In this study, PVDF-PAN/CNT copolymers with different content of MWNTs were fabricated through electrospinning and the solution cast method to obtain new organic semiconductor composites. Their electrical conduction mechanisms are explained by a wide study of temperature dependence of conductivity in the frequency range of 0.5 Hz to 10^4 Hz. Its relationship with blend ratios was investigated by morphology and Fourier transform infrared (FTIR).

Experimental

PVDF, with an average molecular weight of 2.75×10^5 g/mol, and PAN, with a molecular weight of 1.50×10^5 g/mol, were obtained from Sigma Aldrich Co. Dimethylformamide (DMF) was obtained from VWR International LLC. Multi-walled carbon nanotubes (MWNTs-COOH) with a diameter of 10 nm, length from 10–30 micron, and content of –COOH 1.9–2.1 wt.% was supplied by Nanostructured & Amorphous Materials, Inc. USA. The blends were prepared by using electrospinning and the solution cast method in DMF. PVDF-PAN-MWNTs-COOH blended with different weight percent ratios and dispersed in DMF. The solutions were sonicated and stirred, before being poured into glass dishes. They evaporated slowly at room temperature and dried under a vacuum. The solid films continued to dry under the vacuum to remove residual solvent. The electrospinning setup consisted of a plastic syringe (5 mL) and a steel needle. The needle connected to a high voltage power supply. An automatic voltage regulator attached to the power supply to produce uniform voltages. The fiber deposited on an Al sheet on the grounded electrodes, both as a flat sheet

and on a rotating drum. Polymer nanocomposites were electrospun at 15 kV, capillary-screen distances (10 cm) and flow rates (2.5 ml/h).

For the characterization of the samples, a Fourier transform infrared spectrometer (FTIR, Varian 3100) was carried at room temperature. The morphology of the composite was characterized by scanning electron microscopy (SEM) (JSM-6510GS from JEOL), operating with an accelerating voltage of 20 kV.

After drying, the polymer nanocomposites (prepared by electrospinning and the solution cast method) with dimensions 12 mm × 12 mm were sputtered, coated with gold, and sandwiched between two gold plates. The electrical measurements were performed by using a VersaStat MC. Princeton Applied Research at frequency range from 0.5 Hz to 1×10^4 Hz.

Results and discussion

The effect of nanoparticles on morphology and properties of polymer blends have attracted great interest because of the improved physical properties as compared with unmodified polymers. The SEM image of the PVDF/PAN/MWNT-COOH composites prepared by solution cast method are given in Fig. 1.a, which clearly shows highly entangled network-like structure of MWNTs. The percolated MWNTs with network structure and good dispersion are evident in PVDF/PAN-MWNT-COOH composites with 5.47 wt.% of MWNTs. The functionalization of MWNTs increases the compatibility of MWCNTs with PVDF/PAN so as to improve the dispersion of MWNTs in polymer nanocomposites. Compared with the polymer/MWNTs prepared via an in-situ bulk polymerization, the solvent cast film shows a better nanoscopic dispersion of MWNTs[30].

The PVDF-PAN/CNTs fibers interconnected with a large number in different sizes have nonwoven structure. The interconnections of the PVDF/PAN/CNTs fibers increased as the mass content of CNTs in the composite increased. The interconnected network morphology was expected to probable molecular level interactions between C–F (in PVDF) and –CN (in PAN). These molecular interactions induce the phase mixing between PVDF and PAN[31,32]. Fig 1.f. summarized the size distribution of the fiber's diameters processed from different concentrations of MWNTs in PVDF-PAN. It was observed that the average fiber diameter is in the range of 0.03 μm to 1.5 μm. The diameter decreased by increasing the wt.% of CNTs from 1.22 wt% to 7.99 wt% in PVDF-PAN/CNTs nanocomposites[33]. The specific surface area of the MWNTs was higher than that of PVDF-PAN. With a higher specific surface area, the electrostatic interaction of functional groups on the MWNTs can act as nucleating agents in the electrospinning process of polymer nanocomposites. This leads to higher charge density of the electrified jet, forming uniform and much thinner fibers from the polymer solutions containing well-dispersed MWNTs.

In order to understand how the interaction improves the compatibility of the polymer nanocomposite, FTIR analysis was performed. Fig. 2 shows the FTIR spectra of PVDF-PAN-MWNT-COOH prepared by electrospinning and the solution cast method. The FTIR spectra of MWCNT-COOH shows major peaks, located at 2880, 2361–2364, 1700, and 1560 cm^{-1}[34]. The peaks at 2880 and 2361–2364 cm^{-1} are attributed to H–C stretch modes

of H–C=O in the carboxyl group and O–H stretch from strongly hydrogen-bonded –COOH respectively[34]. The peaks at 1700 cm^{-1} and 1560 cm^{-1} are corresponded to carbonyl groups of COOH and the C=C stretch of the COOH in MMWCNTs respectively[34]. Characteristic peak at 2214 cm^{-1} is due to the stretching vibration of the cyano group (–CN), 1454 cm^{-1} for ($–CH_3$) and 1373 cm^{-1} ($–CH_2$), which can be observed in PAN[35]. In addition, FT-IR spectra of composites show bands around 1140–1180 cm^{-1} and 1411–1419cm^{-1}, which are corresponding to the CF_2 bending and CH_2 stretching mode[36], respectively. FTIR results indicate that there are molecular level interactions between the two polymers in the nanofibers. These spectral features give a hint for probable phase mixing between PVDF and PAN.

As shown in Fig 3, the characteristic peaks of the α–phase (non- polar phase) are obtained at 615, 765, and 790 cm^{-1}, while the characteristic peaks of the β–phase (polar phase) are observed at 510, 840 and 1270 cm^{-1}. The occurrence of weak bands for composites prepared by solution cast at 615, 765, and 790 cm^{-1} indicate the presence of a small amount of the α-phase. This is observed by comparing it with polymer nanocomposites prepared by the electrospinning method. It also shows that the beta phase will increase while the alpha phase decrease when there is an increase in CNT content. The intensities of the β–phase became stronger, while the bands of the α-phase became weaker, suggesting that the α–phase is progressively replaced by the β–phase[37,38]. It is well known that the specific surface area of MWNTs is higher than that of PVDF.

This allowed MWNTs to act as nucleating agents in the initial crystallization process of PVDF, leading to a high degree of crystallinity[39]. Under the external electric field in electrospinning, MWNTs can produce inductive charges on the surface, thus lead to a greater Coulomb force during the electrospinning processes. The Coulomb force would then attract part of PVDF chains to the MWNTs surface. The β-phase PVDF would be derivated near the interface during this process. By the electrostatic interaction of functional groups on the MWNTs, which then act as nucleating agents with the polar -CF_2, the PVDF chain will have the zig-zag (T T T T conformation) of the β-phase, instead of the coiled α-phase (TGTG conformation). The characteristic of the γ phase is observed at 1233 cm^{-1}, and can be obtained from strongly polar solvents such as N,N- dimethylformamide (DMF). In the electrospinning process, piezoelectric (β and γ) phases could still be induced via the dipolar/hydrogen interactions between the local polar structure in the crystalline PAN and PVDF[40]. This result is consistent with PVDF/nylon 11 blends[41].

Impedance spectroscopy measurements of the electrical properties for PVDF-PAN/CNTs composites were performed with different concentrations of MWNTs. They had a temperature range of 297–327 K at frequencies between 0.5 Hz and 10^4 Hz. As shown in fig 4a–b the variation of impedance (Z) for the PVDF-PAN/CNTs (prepared by electrospinning and solution cast methods with different concentrations of MWNTs) as a function of frequency at different temperatures. The magnitudes of Z decreased at lower frequencies with increased temperature. At high frequencies, the value of Z merged for all the temperatures of the sample.

The frequency dependent conductivity of the polymer nanocomposite is described by the equation[42,43]:

$$\sigma(\omega) = \sigma_{dc} + A\omega^{n} \quad (1)$$

Where A is the material parameter, n is the frequency exponent in the range of $0 \leq n \leq 1$, σ_{dc} is dc conductivity, and ω is the angular frequency. The conductivities of PVDF-PAN/CNT nanocomposites with different MWNT concentrations as a function of the frequency are presented in Fig.5. The conductivity of PVDF/PAN films showed typical frequency dependence due to the low conductivity of these polymers. With the addition of 1.2 wt.% of MWNTs into the polymer, the frequency dependent AC conductivity with the comparable value to that of PVDF/PAN blend was still preserved. A significant change of the conductivity occurred when the MWCNTs content of the polymer rose from 1.2 wt.% to 5.5 wt.%. The frequency dependent conductivity shows two regions. The plateau region corresponds to the frequency independent dc conductivity (i.e., σ_{dc}) and the dispersive region corresponds to the frequency dependent part[44]. It was confirmed by a typical fit of the above equation to the experimental data shown in figure 5 that the value of n was in the range from 0.48993 to 0.8752 for the samples prepared by solution cast method and in the range from 0.861 to 0.90475 for the samples prepared by the electrospinning method. These results reveal the semiconductor behaviors of the composites[45]. It is evident from the results that none of the CNT composites displayed the ideal dielectric behavior exhibited by the pure PVDF/PAN, however the samples ranged from pure dielectric to clear semiconductor behavior as the content of CNTs in the material decreased. For very thin samples (for example 1 mm), the frequency independence of the impedance modulus is suggestive of an ohmic material that must exhibit a very well connected nanotube network. When the loading of the CNTs in the material increased, it appeared that the uniformity of materials started playing a more significant role which made it difficult for the nanotubes to arrange themselves into an interconnected 3D net.

The relationship between the electrical conductivity of the PVDF-PAN/CNT composites and the temperature is on display in Fig. 6. As seen in Fig. 6, the electrical conductivity of the composites increased with temperature. The conductivity of the nanocomposites were analyzed according to the well-known Arrhenius equation[46]:

$$\sigma = \sigma_{o} \exp\left[\frac{-E_{a}}{kT}\right] \quad (2)$$

Where E_a is the conductivity activation energy, K is the Boltzman constant and σ_o is the pre-exponential factor, which includes the charge carrier mobility and density of state. The semi logarithmic plots of $\ln(\sigma)$ vs. T^{-1} are linear with conductivity activation energy, E_a, values of 112 meV and 282 meV for PVDF/PAN and PVDF-PAN/CNTs, respectively.

The corresponding values of the activation energies are in Table 1. It clearly showed that the electrical conductivity of PVDF-PAN/MWCNTs, prepared by the electrospinning method,

increased from 5.7×10^{-7} S/cm to 1.31×10^{-5} S/cm with the increase of MWCNTs content. On the other hand, when the content of CNTs in the nanocomposites increased, the electrical conductivity of PVDF-PAN/CNTs prepared by the solution cast method increased from 8.6×10^{-7} to 2.33×10^{-5} S/cm.

Figure 7 presents the conductivity of PVDF-PAN/CNT composites prepared by using electrospinning and solution cast methods as a function of the MWNTs contents. The electrical conductivity as a function of MWNTs showed the order of 5.7×10^{-7} S/cm to 1.23×10^{-6} S/cm at 24°C. The conductivity of PVDF-PAN/CNTs was compared using the electrospinning method and the solution cast method at the same wt.%. The conductivity by the solution cast method had a higher conductivity (9.18×10^{-6} S/cm) than the conductivity by the electrospinning method (2.09×10^{-6} S/cm). Similar results were reported by Yu et al. [47]. It was determined that the electrical conductivity of pristine SWCNTs/epoxy composites were several orders higher than that of carboxylic functionalized SWCNTs/epoxy composites with the same SWCNTs content.

It was observed that the addition of MWNTs into PVDF/PAN could enhance the conductivity of the studied polymer with an increased MWNT percentage; however, the phase transformation encouraged a change of conduction mechanism. The polymer nanocomposites with a high α-phase demonstrated a clear percolating behavior on the measured conductivity with high values for the percolation threshold. By the electrostatic interaction of functional groups on the MWNTs with the polar-CF_2, the PVDF chain will have the zig-zag conformation of the β-phase, instead of the coiled α-phase conformation. The polymer nanocomposites with high β- phase exhibits typical ionic conduction behavior due to the breaking of percolation paths associated to the structural and morphological changes. The obtained electronic parameters prove that PVDF-PAN/CNTs exhibit organic semiconductor behavior. In particular, compared with other spherical-shaped conductive filling materials such as carbon black. CNTs with large length/diameter aspect ratios help the composites system show a high electric conductivity at low concentrations due to their low percolation threshold[48,49]. However, carabineiro *et al.*[50] observed that the conductivity of the PVDF-MWNT further increased by nearly three orders of magnitude, from order of 10^{-7} S/cm to order of 10^{-4} S/cm, by the increased concentration of the MWNTs.

Figure 8 shows typical galvanostatic discharge of PVDF-PAN/CNTs with different currents and wt. % of MWNTs. It showed that the potential decreased exponentially, nearly to zero. The discharge time of polymer nanocomposites increased with the increase of MWNTs content.

Galvanostatic discharge curves (Figs. 8a–b) were used to determine the capacitance of the polymer composite electrodes. The specific capacitance per mass of one pellet electrode was calculated according to the equation:

$$C_{sp} = \frac{I \times \Delta t}{\Delta E \times m} \quad (3)$$

Where I is the discharge current in amperes, Δt is the discharge time in seconds corresponding to the voltage difference ΔE in volts, and m is the mass in grams. It was found that, the specific capacitance increased from 0.2 F/g to 8 F/g by increasing the current density and wt. % of MWNTs. The specific power (SP) and specific energy (SE) were calculated from charge-discharge cycling data using the following relationships[51]:

$$\text{Specific Power } (\frac{\text{W}}{\text{kg}}) = \frac{\text{I} \times \Delta\text{E}}{\text{m}} \quad (4)$$

$$\text{Specific Energy } (\frac{\text{Wh}}{\text{kg}}) = \frac{\text{I} \times \Delta\text{E} \times \text{t}}{\text{m} \times 3600} \quad (5)$$

Where I, *t, and m* are the discharge current in amperes, discharge time in seconds, and mass of PVDF-PAN/CNTs in kg, respectively. The calculated *SP* and *SE* values are shown in Fig. 9 (Ragon plot). It is found that the largest specific energy for PVDF/PAN of 15.57 Wh/kg was obtained at a corresponding specific power of 560.3 W/kg and the largest specific energy for PVDF-PAN/CNTs (with 5.58 wt.% of MWNTs) of 129.7 Wh/kg was obtained at a corresponding specific power of 4671 W/kg.

It was noticed that the specific energy of the PVDF-PAN/CNTs increased from 15.57 Wh/kg to 129.7 Wh/kg after the addition of MWNTs. It was several times higher than that of the polymer blend without MWNTs. It is clear that the PVDF-PAN/CNTs have high performance electronic components. These characteristic properties of obtained polymer nanocomposites will prove to be an optimal candidates for many applications such as nanogenerators, organic semiconductors, transducers and electrical energy storage[52].

Conclusions

PVDF/PAN/MCNTs nanocomposites with different contents of MWNTs were successfully prepared through electrospinning and the solution cast method. FTIR results indicate that MWNTs act as a nucleation agent during crystallization and slightly increased the β–phase crystal and could decrease the α-phase in the PVDF/PAN/MWNT-COOH nanocomposites. The morphological properties and electrical conductivity of polymer nanocomposites have been analysed. The results showed that the nanocomposites prepared by the solution cast method had a much higher conductivity (9.18×10^{-6} S/cm) than the nanocomposites prepared by the solution cast method (2.09×10^{-6} S/cm) at the same MWNT content. In conclusion, the MWNTs play a very important role in both structural and electrical properties of the composites. The polymer nanocomposites can be useful for applications such as nanogenerators, organic semiconductors, transducers and electrical energy storage.

Acknowledgments

Z.Wang. would like to acknowledge NIH funding for this work via Grant Number NIH 2G12MD007595-06, NIMHD grant number 5G12MD007595 and NIGMS grant number 8UL1GM118967. This work also supported by the Louisiana Cancer Research Consortium (LCRC).

References

1. Stankovich S, Dikin DA, Dommett GH, Kohlhaas KM, Zimney EJ, Stach EA, Piner RD, Nguyen ST, Ruoff RS. Nature. 2006; 442:282. [PubMed: 16855586]
2. Wu M, Shaw L. Journal of applied polymer science. 2006; 99:477.
3. Yuen SM, Ma CCM, Chiang CL, Lin YY, Teng CC. Journal of Polymer Science Part A: Polymer Chemistry. 2007; 45:3349.
4. Aqeel SM, Küçükyavuz Z. Journal of Applied Polymer Science. 2011; 119:142.
5. Aqeel SM, Wang Z, Than L, Sreenivasulu G, Zeng X. RSC Advances. 2015; 5:76383. [PubMed: 26989486]
6. Wang Z, Colorad HA, Guo Z-H, Kim H, Park C-L, Hahn HT, Lee S-G, Lee K-H, Shang Y-Q. Materials Research. 2012; 15:510.
7. Agarwal, A., Bakshi, SR., Lahiri, D. Carbon nanotubes: reinforced metal matrix composites. CRC press; 2016.
8. Wang Z, Lu M, Li H-L, Guo X-Y. Mater Chem Phys. 2006; 100:77.
9. Zhang L, Zhang Q, Xie H, Guo J, Lyu H, Li Y, Sun Z, Wang H, Guo Z. Applied Catalysis B: Environmental. 2017; 201:470.
10. Wei H, Cui D, Ma J, Chu L, Zhao X, Song H, Liu H, Liu T, Wang N, Guo Z. Journal of Materials Chemistry A. 2017
11. Huang B, Wang Z, Chen L, Xue R, Wang F. Solid State Ionics. 1996; 91:279.
12. Tatsuma T, Taguchi M, Iwaku M, Sotomura T, Oyama N. Journal of Electroanalytical Chemistry. 1999; 472:142.
13. Nalwa, HS. Ferroelectric Polymers: Chemistry: Physics, and Applications. CRC Press; 1995.
14. Ducharme S, Reece TJ, Othon CM, Rannow RK. Device and Materials Reliability, IEEE Transactions on. 2005; 5:720.
15. Naber RC, Asadi K, Blom PW, de Leeuw DM, de Boer B. Advanced materials. 2010; 22:933. [PubMed: 20217816]
16. Guan F, Pan J, Wang J, Wang Q, Zhu L. Macromolecules. 2009; 43:384.
17. Guan F, Yuan Z, Shu EW, Zhu L. Applied Physics Letters. 2009; 94:052907.
18. Sreekumar TV, Liu T, Min BG, Guo H, Kumar S, Hauge RH, Smalley RE. Advanced Materials. 2004; 16:58.
19. Ko F, Gogotsi Y, Ali A, Naguib N, Ye H, Yang G, Li C, Willis P. Advanced materials. 2003; 15:1161.
20. Prilutsky S, Zussman E, Cohen Y. Journal of Polymer Science Part B: Polymer Physics. 2010; 48:2121.
21. Aqeel SM, Wang Z, Than L, Sreenivasulu G, Zeng X. RSC Advances. 2015; 5:76383. [PubMed: 26989486]
22. Huang J, Cao Y, Huang Z, Imbraguglio SA, Wang Z, Peng X, Guo Z. Macromolecular Materials and Engineering. 2016; 301:1327. [PubMed: 29104455]
23. Guan X, Zheng G, Dai K, Liu C, Yan X, Shen C, Guo Z. ACS applied materials & interfaces. 2016; 8:14150. [PubMed: 27172292]
24. Ghafari E, Feng Y, Liu Y, Ferguson I, Lu N. Composites Part B: Engineering. 2017; 116:40.
25. Heikkilä P, Harlin A. European Polymer Journal. 2008; 44:3067.
26. Huang Z-M, Zhang Y-Z, Kotaki M, Ramakrishna S. Composites science and technology. 2003; 63:2223.
27. Varesano A, Carletto RA, Mazzuchetti G. Journal of Materials Processing Technology. 2009; 209:5178.
28. Kim JS, Reneker DH. Polymer Engineering & Science. 1999; 39:849.
29. Fang X, Reneker D. Journal of Macromolecular Science, Part B: Physics. 1997; 36:169.
30. Park SJ, Cho MS, Lim ST, Choi HJ, Jhon MS. Macromolecular rapid communications. 2005; 26:1563.

31. Dong H, Nyame V, MacDiarmid AG, Jones WE. Journal of Polymer Science Part B: Polymer Physics. 2004; 42:3934.
32. Gopalan AI, Santhosh P, Manesh KM, Nho JH, Kim SH, Hwang C-G, Lee K-P. Journal of Membrane Science. 2008; 325:683.
33. Yu H, Huang T, Lu M, Mao M, Zhang Q, Wang H. Nanotechnology. 2013; 24:405401. [PubMed: 24029779]
34. Sahoo NG, Bao H, Pan Y, Pal M, Kakran M, Cheng HKF, Li L, Tan LP. Chemical Communications. 2011; 47:5235. [PubMed: 21451845]
35. Trchová M, Šeděnková I, Tobolková E, Stejskal J. Polymer Degradation and Stability. 2004; 86:179.
36. Vasundhara K, Mandal BP, Tyagi AK. RSC Advances. 2015; 5:8591.
37. Song R, Yang D, He L. Journal of Materials Science. 2007; 42:8408.
38. He L, Sun J, Wang X, Yao L, Li J, Song R, Hao Y, He Y, Huang W. Journal of colloid and interface science. 2011; 363:122. [PubMed: 21821257]
39. Bao S, Liang G, Tjong SC. Carbon. 2011; 49:1758.
40. Zhong G, Zhang L, Su R, Wang K, Fong H, Zhu L. Polymer. 2011; 52:2228.
41. Gao Q, Scheinbeim JI. Macromolecules. 2000; 33:7564.
42. Almond D, West A. Solid State Ionics. 1987; 23:27.
43. Jonscher AK. Nature. 1977; 267:673.
44. Barik SK, Choudhary R, Singh A. Advanced Material Letter. 2011; 2:419.
45. Kim D, Kim Y, Choi K, Grunlan JC, Yu C. ACS nano. 2009; 4:513.
46. Kang SD, Snyder GJ. Nature Materials. 2016
47. Yu A, Itkis ME, Bekyarova E, Haddon RC. Applied Physics Letters. 2006; 89:133102.
48. Du J, Zhao L, Zeng Y, Zhang L, Li F, Liu P, Liu C. Carbon. 2011; 49:1094.
49. Kovacs JZ, Velagala BS, Schulte K, Bauhofer W. Composites Science and Technology. 2007; 67:922.
50. Carabineiro S, Pereira M, Nunes-Pereira J, Silva J, Caparrós C, Sencadas V, Lanceros-Méndez S. Journal of Materials Science. 2012; 47:8103.
51. Reddy ALM, Ramaprabhu S. The Journal of Physical Chemistry C. 2007; 111:7727.
52. Wang Q, Zhu L. Journal of Polymer Science Part B: Polymer Physics. 2011; 49:1421.

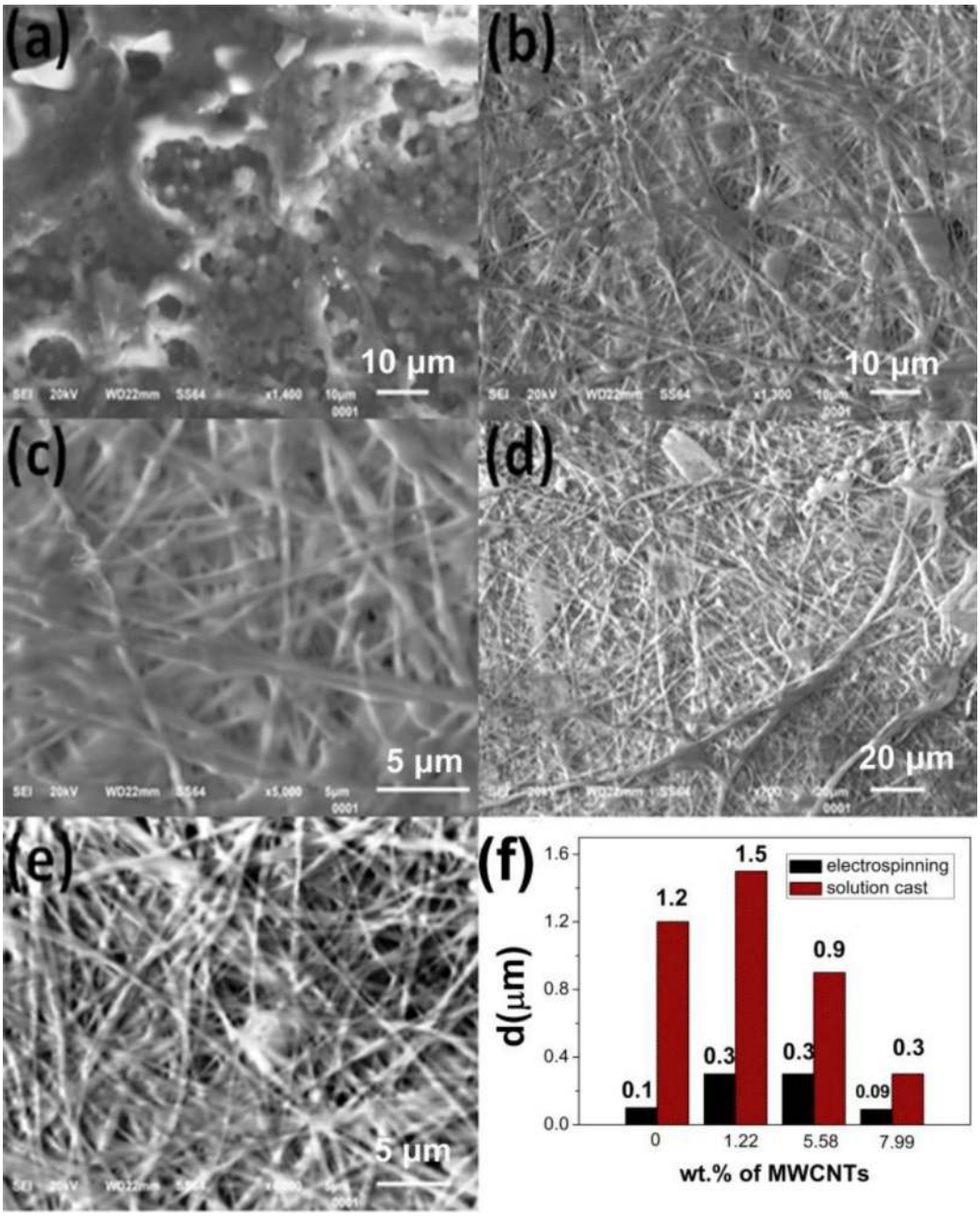

Fig.1.

SEM images of the PVDF-PAN-MWNT-COOH composites prepared by solution cast method with 5.47 wt. %. of MWNT (a) and electrospinning method with 5.58 wt. %. of MWNTs (b and c) and with 7.99 wt. %. of MWNT (d and e). f: The size distribution of PVDF-PAN-MWNT-COOH fibers prepared by solution cast and electrospinning method as a function of MWNTs content.

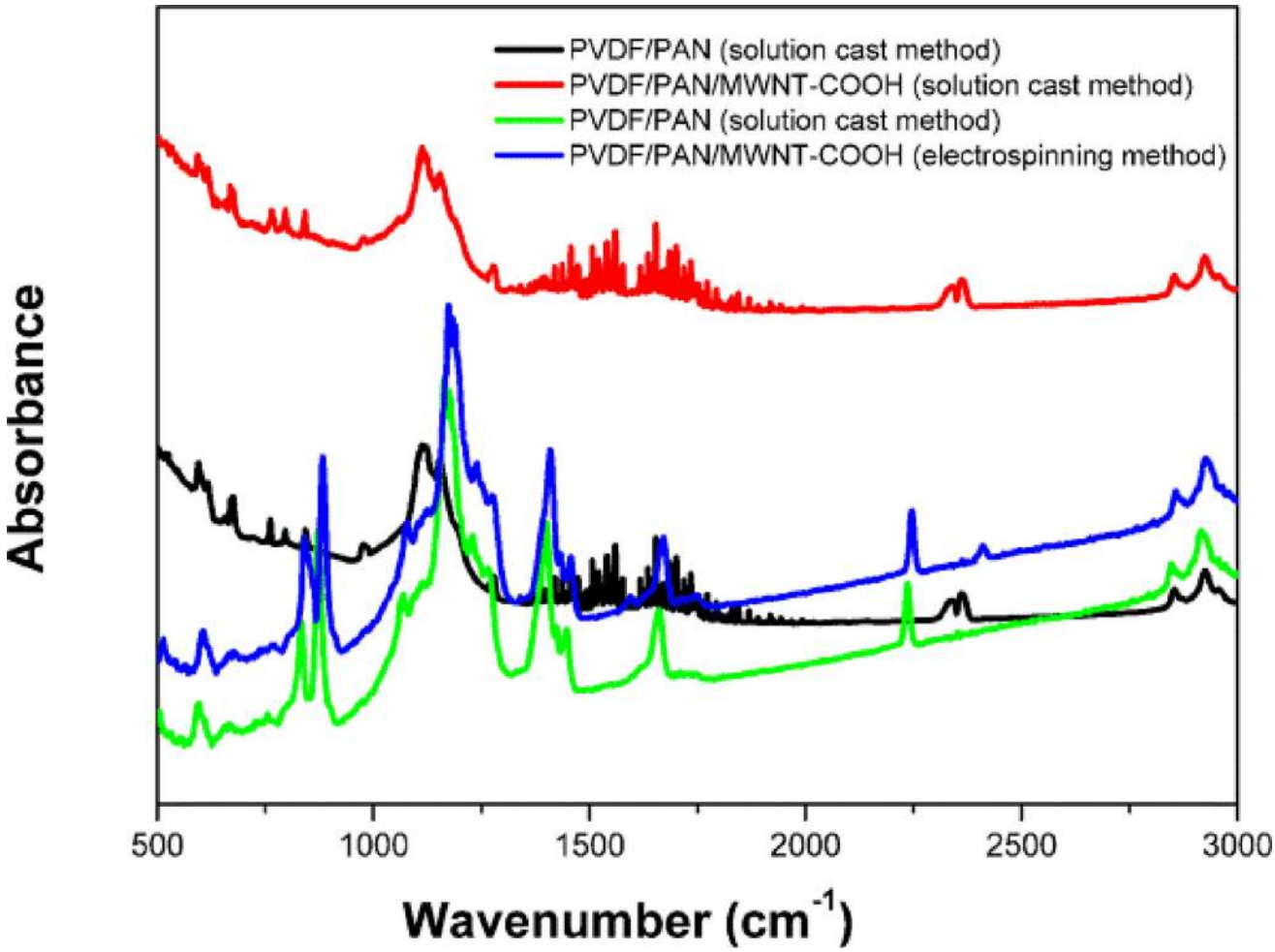

Fig.2.

FTIR spectra of PVDF/PAN and PVDF-PAN/CNTs composites prepared by solution cast and electrospinning methods.

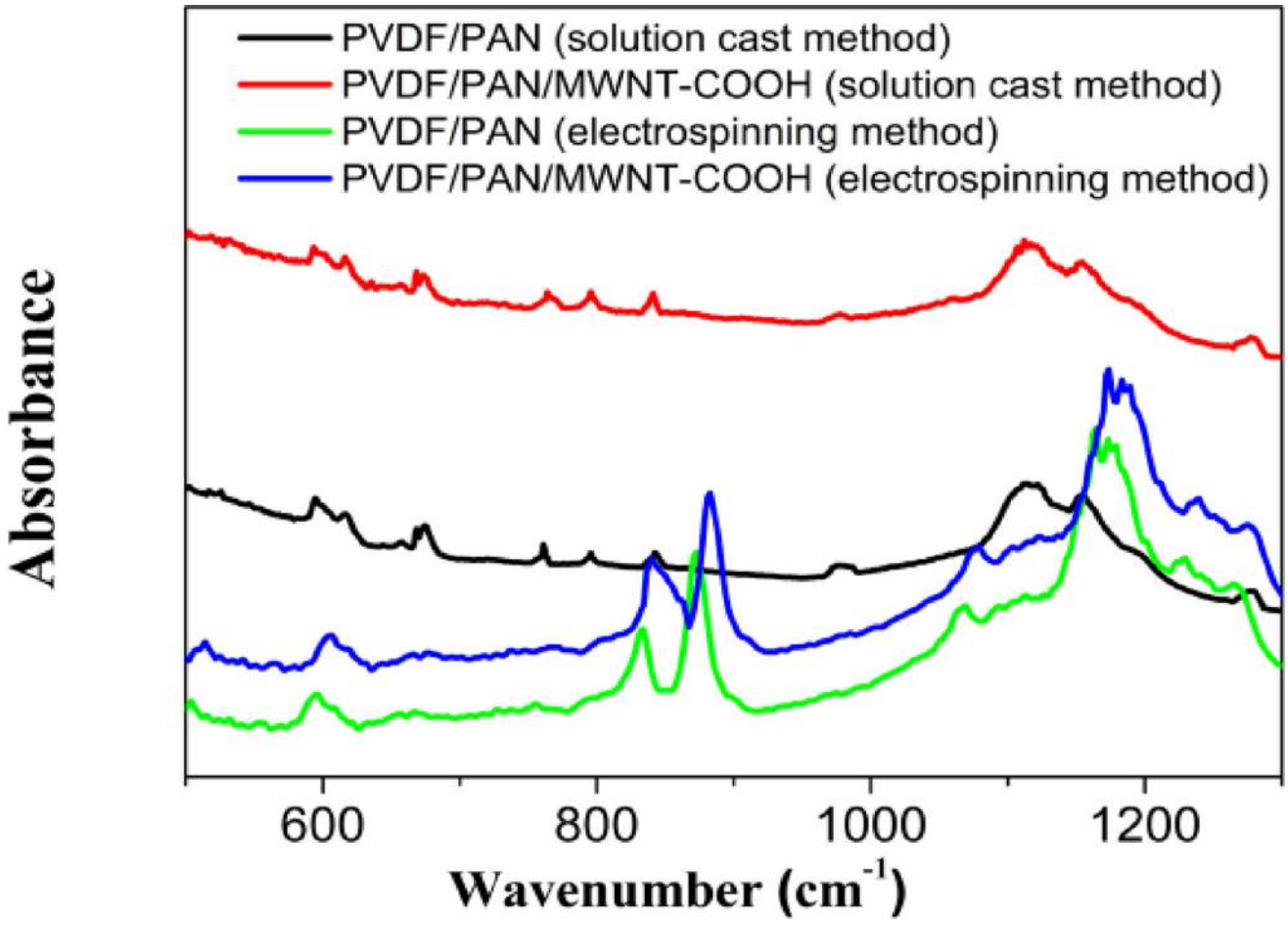

Fig.3.

FTIR spectra, α and β formation of PVDF/PAN and PVDF-PAN/MWCNTs nanocomposites prepared by solution cast and electrospinning methods

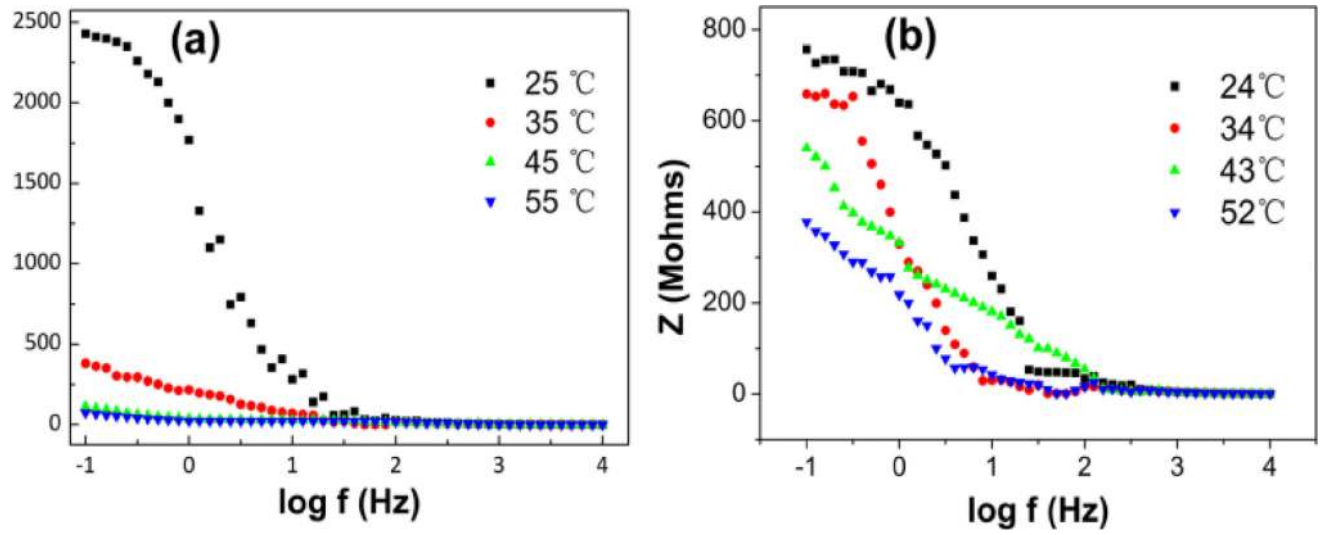

Fig.4.

The impedance (Z) for the PVDF-PAN/CNTs prepared by electrospinning method (a) and PVDF-PAN/CNTs prepared by solution cast method (b) as a function of frequency.

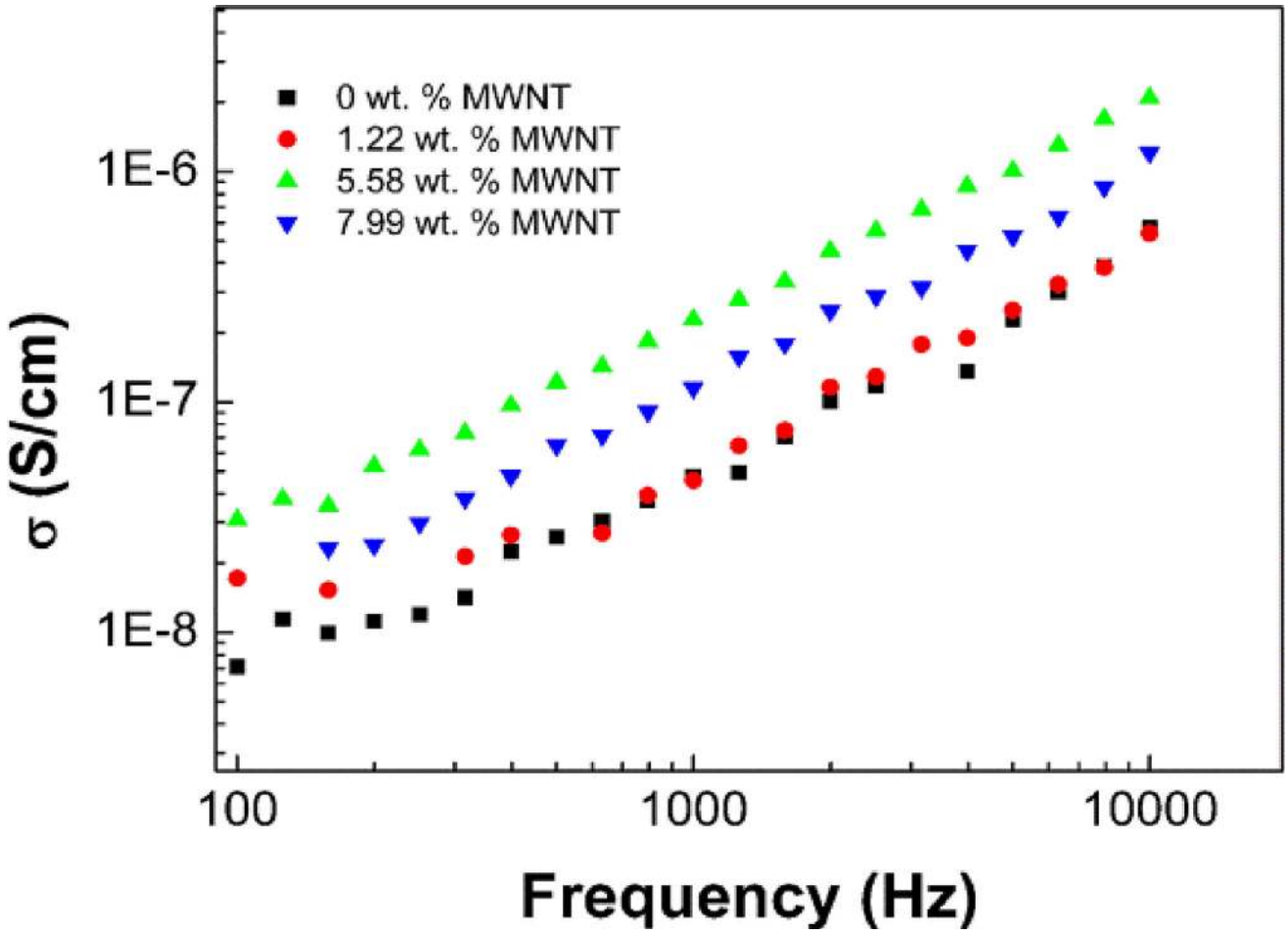

Fig.5.
The conductivity for the PVDF-PAN/CNTs (prepared by the electrospinning method) as a function of frequency.

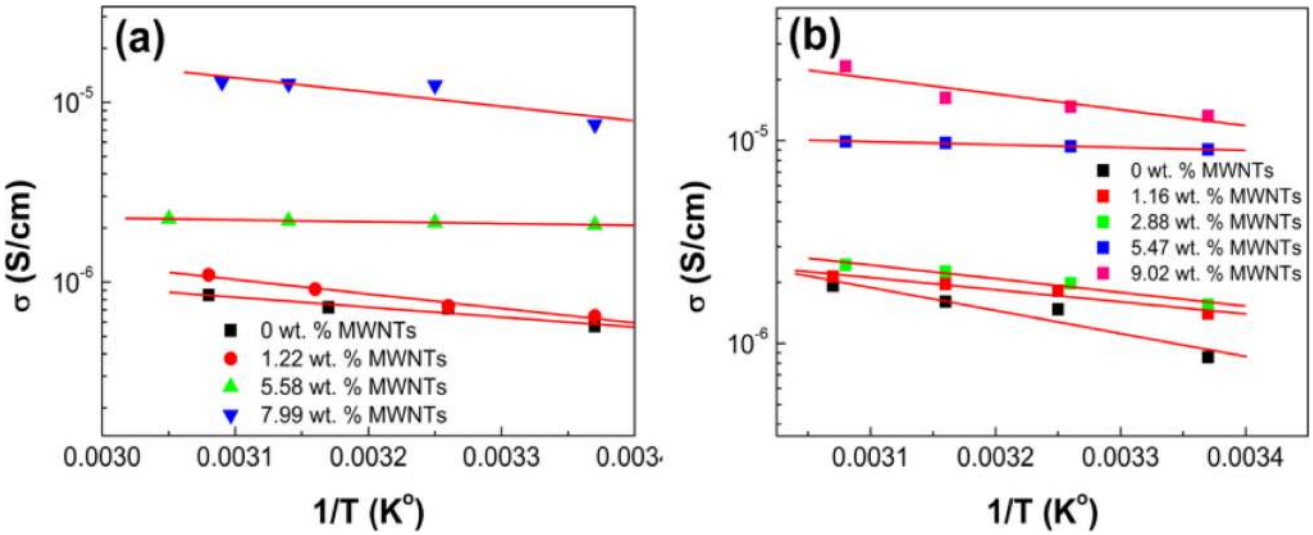

Fig.6.

Arrhenius plots of the PVDF-PAN/MWCNTs composites prepared by electrospinning method (a) and prepared by solution cast method (b) with different content of MWCNTs.

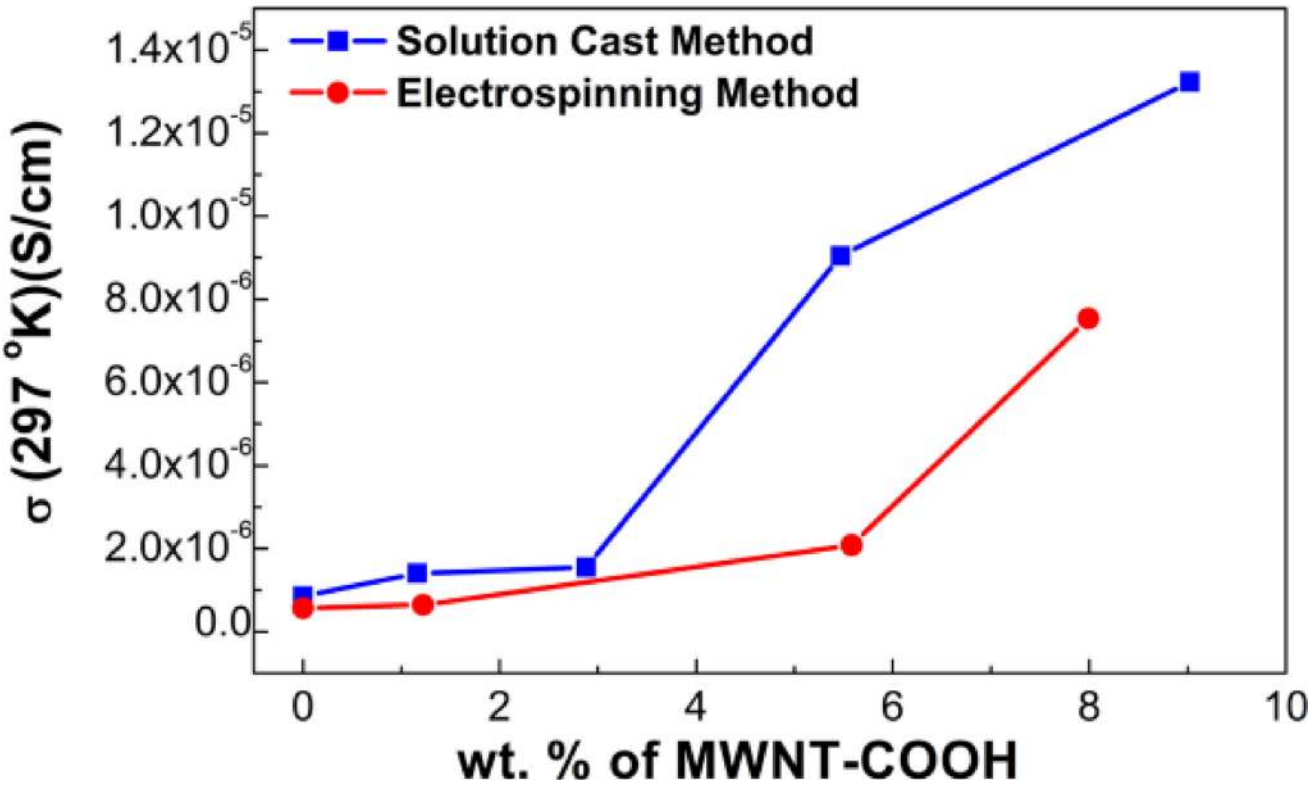

Fig.7.
Electrical conductivity of the PVDF-PAN/CNTs composites as a function of the MWNT content.

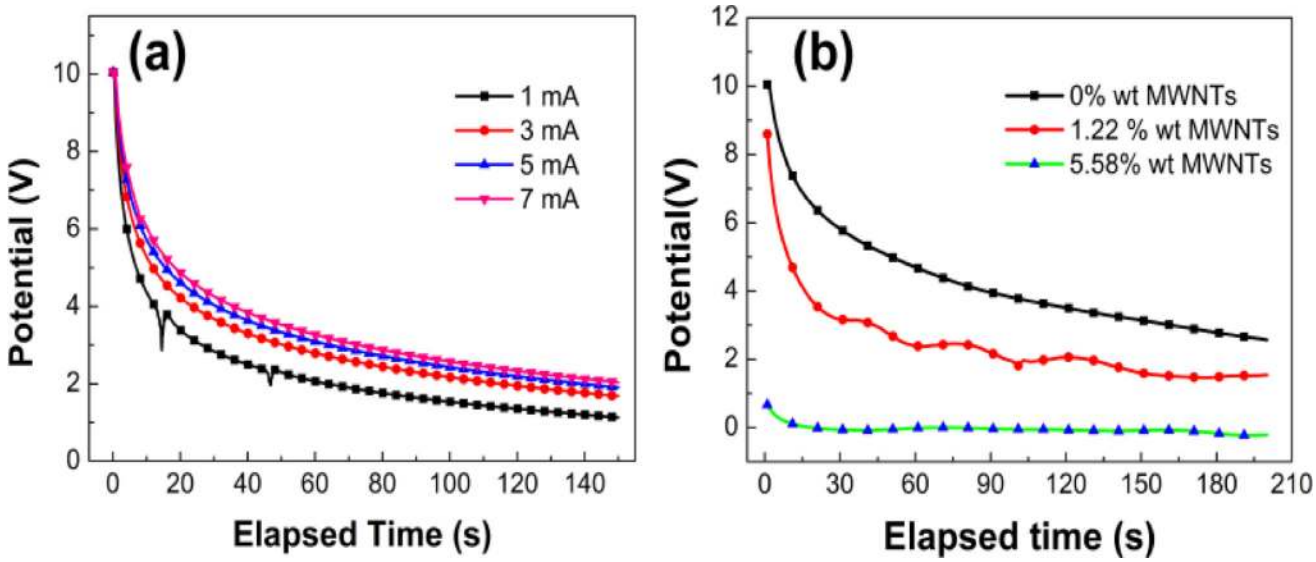

Fig.8.

Galvanostatic discharge of PVDF-PAN/CNTs prepared by electrospinning method (a) and prepared by electrospinning method (b) at different currents and different wt. % of MWNTs.

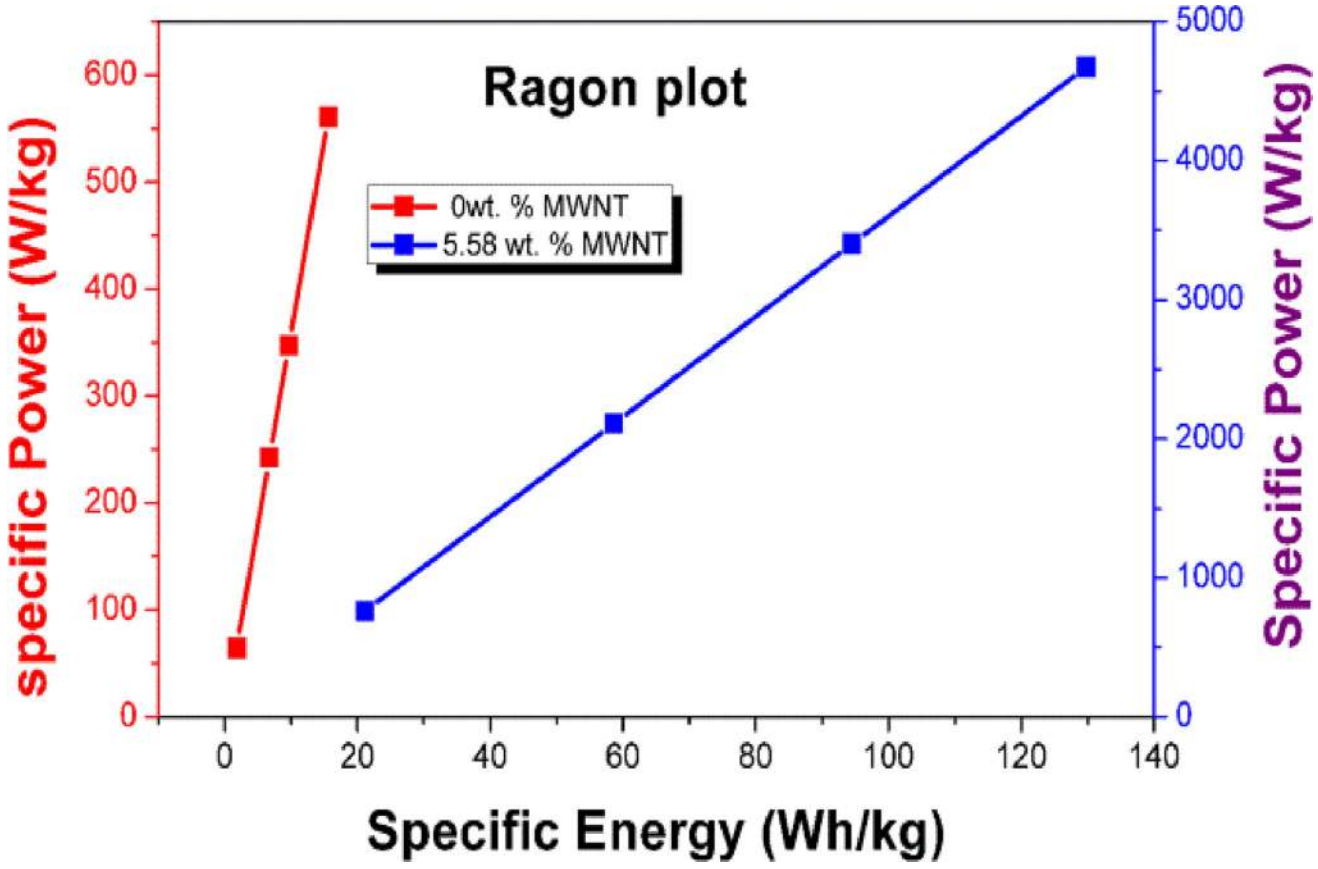

Fig.9.

Plot of specific power vs. specific energy (Ragon plots) for PVDF-PAN/CNTs composite (prepared by electrospinning method).

Table 1

Arrhenius Activation Parameters for the PVDF-PAN/CNTs prepared by the electrospinning method and the solution cast method.

Electrospinning Method			Solution Cast Method		
Wt.% of MWNTs	**σ_0 [mS/cm]**	**E_a [meV]**	**Wt.% of MWNTs**	**σ_0 [mS/cm]**	**E_a [meV]**
0	0.045	112	0	6.61	127
1.22	0.333	161	1.16	0.165	121
5.58	0.0046	20.5	2.88	0.311	135
7.99	5.36	166	5.47	0.027	282
			9.02	5.92	158